ULTRAFAST FORMATION OF HYDRATED ELECTRONS IN WATER AT HIGH CONCENTRATION: EXPERIMENTAL EVIDENCE OF THE FREE ELECTRON

P. Palianov[a]*, *P. Martin*[b]**, *F. Quéré*[b], *S. Pommeret*[c]

[a] *Institute of High Current Electronics, Siberin Branch, Russian Academy of Sciences*
634055, Tomsk, Russia

[b] *Service des Photons, Atomes et Molécules*
[c] *Service Interdisciplinaire sur les Systèmes Moléculaires et les Matériaux, UMR 3299 CNRS*

Commissariat à l'Energie Atomique et aux Energies Alternatives, DSM/IRAMIS, CEA/Saclay,
91191 Gif sur Yvette, France

Using a time-resolved optical interferometric technique, we investigate the ultrafast primary events following the interaction of an ultrashort laser pulse with pure water in the TW/cm^2 regime. Because our method is sensitive to the quasi-instantaneous electron energy level position, we demonstrate that in contrast to the well-known low-intensity regime, where the free electrons are instantaneously captured by pre-existing traps, in this new regime of excitation, free electrons are clearly observed, exhibiting a substantial contribution in the near IR. The delayed localization is attributed to the saturation of pre-existing cavities in the liquid by the large number of the excited electron states created.

The solvated electron appears in a variety of polar liquids and is created as soon as an electron is injected into the solvent. This chemical species has been thoroughly studied experimentally and theoretically [1–4] because it is recognized to take part in a very large class of aqueous chemical reactions. The solvated electron has been particularly studied in water because of its key role in biology, chemistry, and physics. It can be generated by several different mechanisms, e. g., radiolysis, electrochemical, or optical excitation. The equilibrated solvated electrons, whose ground state survives for some hundreds of nanoseconds [5], resides in an approximatively spherical solvent cavity made with six water molecules with one of their OH bond pointing toward the cavity center [6, 7], as was recently confirmed by Car Parinello molecular dynamics studies [8, 9]. Its spectral properties, first reported in the early 1960s, exhibit a broad asymmetric absorption band centred at 1.75 eV [10], which has been intensively studied since

its discovery [11]. The ground state of this spherical trap has an s-like character and a set of three nearly degenerate p-like excited states [6, 7, 12] correspond to its first excited state.

To gain a better understanding of the nature of the electron–water interactions, two types of experiment have mainly been realized up to now: i) time-resolving the transient absorption in pure liquid water from the injection of electrons in the conduction band up to the full solvation [13–15] and ii) measuring the absorption on the equilibrated solvated electron [16, 17]. We note that all these experiments have been done using the same ultrafast time-resolved visible–infrared absorption spectroscopy techniques at "low" pump power densities (a few GW/cm^2). The infrared absorption spectrum [18] and the Raman spectrum [19] of the hydrated electron have been measured, which is in favor of the first-principle molecular dynamics [8, 9].

In this paper, we clarify the very early stages of the formation of the solvated electron by using another technique allowing a direct and simultaneous measurement of the variation of the real and the imaginary part (absorption) of the refractive index with a tem-

*E-mail: palianov@yandex.ru
**E-mail: philippe.martin@cea.fr

poral resolution better than 50 fs. The main advantage of this interferometric-based techniques, is that it permits following the instantaneous position of the energy level of the electron in real time [20]. Contrary to most of the previous studies, the present one has been performed at very high pump power, producing an extremely high concentration of hydrated electrons (up to the molar regime) [21, 22]. In a sense, what we mimic is closer to what occurs in dense tracks of radiation chemistry [1]. The experimental setup has already been described in detail [20, 23] and we only briefly recall the principle of the measurements. The probe system consists of two identical pulses separated by a fixed time delay and collinearly propagating. One (the reference pulse) crosses the sample before the pump pulse and the other (the probe pulse) after it. The reference and probe pulses are sent into a spectrometer, and the perturbed region in the sample is imaged at the entrance slit.

The modification of the refractive index Δn induces a phase shift $\Delta \Phi$ for the probe pulse, which is proportional to the length L over which the pump and probe beams overlap. The phase shift is given by

$$\Delta \Phi(t) = \frac{2\pi L}{\lambda} \operatorname{Re}(\Delta n(t)),$$

where λ is the probe beam wavelength and $\Delta n(t) = n(t) - n_0$ is the instantaneous change of the refractive index that results from the pump-induced excitation (n_0 is the unperturbed refractive index). By using the contrast of the fringes, we obtain the change in the absorption coefficient, i. e., in the imaginary part of the refractive index. This can be written explicitly as

$$A = 1 - \exp\left[-\frac{2L\omega}{c} \operatorname{Im}(n(t))\right].$$

Both quantities (the phase shift and absorption) are obtained by a Fourier analysis of the interference image at the output of the spectrometer. The laser with the titanium-doped sapphire (Ti-Sa) deliver 60-fs pulses with energies up to 100 mJ. We use a part of the laser beam with fundamental wavelength (800 nm, 1.55 eV photons) as a probe and the pump beam after the frequency doubling (395 nm) is spatially filtered, to produce a soft Gaussian profile. Typically, we used pulse energies in the 0.4 mJ range accommodating shot-to-shot fluctuations of about 10 %.

The pump and probe arrangement is shown in Fig. 1. The water being contained in a quartz cell, the main difficulty was to avoid some possible spurious contributions from the cell itself. Of course, it has been checked that without water in the cell, no fringe
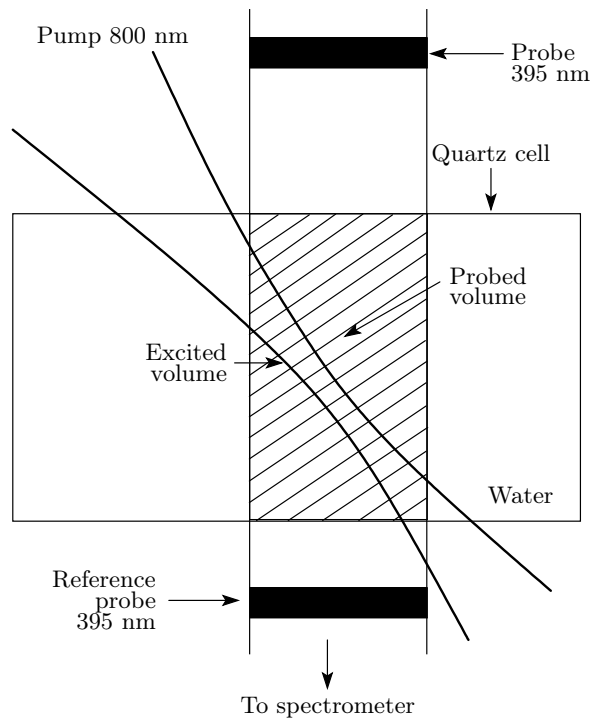
Fig. 1. Schematic view of the pump and probe arrangement. The intensity in the middle of the cell is $4 \cdot 10^{12}$ W/cm^2, the intensity at the surface of the cell is 10^9 W/cm^2

distortion was visible on the CCD camera. We used a very short focal lens (10 cm) adjusting the focal point in the center of the cell, where the intensity was close to $4 \cdot 10^{12}$ W/cm^2, whereas the intensity at the surface of the cell was lower than 10^9 W/cm^2. This intensity in water was set slightly bellow the filamentation or white light generation regime. In practice, the window where the signal is unambiguously distinguishable from the quartz cell and below the breakdown of water was very thin, impeding experiments of varying the pump intensity over large ranges.

The temporal behavior of the phase shift $\Delta \Phi$ and the corresponding absorption $\ln(I_0/I_t)$, where I_0 (I_t) is the intensity of the probe beam passing through unperturbed (perturbed) water, are shown, after a spatial integration along the slit of the spectrometer, in Fig. 2. We present all shots without discrimination or averaging. The relative spreading of the data points corresponds to exact error bars. This spreading occurs, because several shots at higher intensities due to shot-to-shot energy fluctuations, induce the breakdown of water, producing spurious phase shifts in the interference pattern. In these graphs, the zero delay cor-
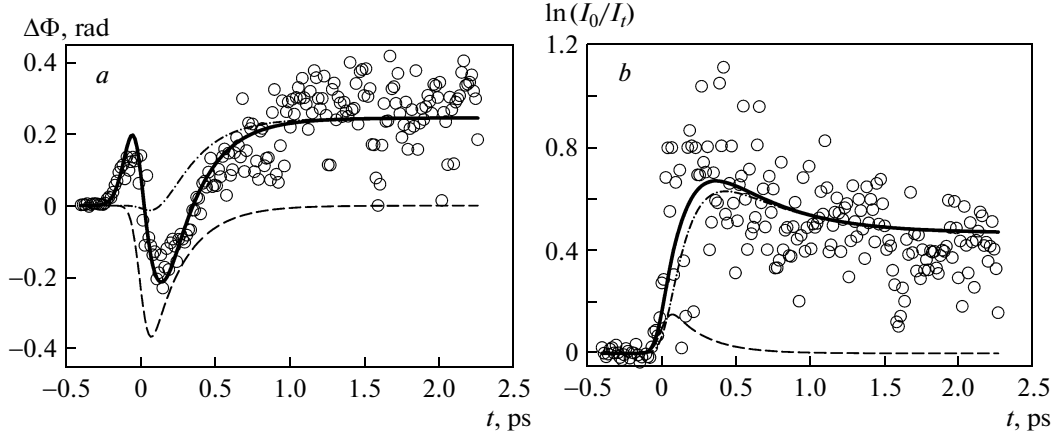
Fig. 2. (a) Phase shift and (b) absorption of the probe pulse as functions of delay time in pure water. The incident pulse intensity is 2.2 TW/cm^2 and the probe pulse wavelength is 1.57 eV. Circles correspond to the single-shot experiment; full thick lines to the simulation based on the Drude–Lorentz model; dashed lines to the free-electron contribution; dash-and-dot-lines to the trapped electron contribution

responds to the maximum overlap between the probe and the pump envelop pulses. In Fig. 2a, we first observe a positive phase shift (for negative delay times), immediately followed by a negative one (for small positive delay times). After roughly 400 fs, the phase shift becomes positive and slowly increases to a steady-state value within the time window under consideration. The behavior of absorption (Fig. 2b) is less complicated: we first observe a very abrupt increase right after the pump pulse, followed by a relaxation on the same time scale as the increase in the phase observed in Fig. 2a. We note that the maximum absorption is reached approximately 400 fs after the pump pulse. A similiar behavior was already observed for the transient absorption at high pump power densities with a pump wavelength of 400 nm [22] or 266 nm [21].

To interpret our results, we use the Drude–Lorentz model. This is basicaly a two-level system in which, in order to preserve the "band structure" and retain the validity of the model, the condition is imposed that the number of excited electrons be small compared to the total number of electrons available in the liquid ($3.3 \cdot 10^{22}$ cm^{-3}). As we see in what follows, this requirement is perfectly satisfied. The Drude–Lorentz model can be written as

$$\Delta n(t) = n_2 I_p(t) + \frac{e^2}{2n_0\varepsilon_0} \frac{-N^{free}(t)}{(\omega^2 - i\omega/\tau^{free})m^*} + $$
$$ + \frac{N^{trap}(t)}{(\omega^2_{trap}(t) - \omega^2 - i\omega W^{solv}/\hbar)m_e}, \quad (1)$$

where e is the electron charge, m_e is its mass, m^* its reduced mass in the conduction band, ε_0 is the vacuum permittivity, $1/\tau^{free}$ is the collision rate of the excited free electrons, W^{solv} is the width of the optical absorption spectra of solvated electrons, n_0 is the refractive index, n_2 is the nonlinear refractive index, $\omega_{trap}(t)$ is the absorption frequency of the trapped electron, $N^{free}(t)$ is the number of free electrons, and N_{trap} is the number of trapped electrons.

The first term in Eq. (1) represents the Kerr effect. It is proportional to the (Gaussian) pump laser intensity $I_p(t)$ and contributes positively to the phase shift because the nonlinear index n_2 is positive (it was estimated in [24] to be in the range $(0.5–1.0) \cdot 10^{-15}$ cm^2/W). This is observed in all dielectric materials and lasts as long as the pump and the probe pulses overlap in the sample. The real part of the second term (the "free electron" or "plasma" term), which is proportional to the density $N^{free}(t)$ of free electrons created by the pump pulse, is always negative. The real part of the last term stands for the trapping (followed by solvation) of the electrons, $N^{trap}(t)$. Its sign is determined by the relative values of ω_{trap} and ω. For example, in the case of shallow traps ($\omega_{solv} < \omega$), its contribution is negative. This means that the phase shift measurement alone is insufficient to distinguish between the electrons in the conduction band and the electrons in shallow traps. On the contrary, if the absorption bands associated with the trapped state correspond to wavelengths shorter than the probe wavelength ($\omega_{solv} > \omega$), the trapping of electrons (solvation)

Table. Parameters used in the simulation

Parameter	Value	Fitted
n_0	1.5	No
N_0, cm^{-3}	$3.3 \cdot 10^{22}$	No[a]
τ^{free}, fs	1.85	No[b]
ω_{hyd}^{∞}, eV	1.72	No [10]
W^{solv}, eV	0.34	No[c]
σ^3, cm$^6 \cdot$s^2	$2.8 \cdot 10^{-81}$	No [22]
η	0.42	No [22]
ω_{trap}^0, eV	1.52	Yes
τ^{solv}, fs	450	Yes
τ^{trap}, fs	230	Yes
m^*/m_e	0.18	Yes
n_2, cm^2/W	$6.2 \cdot 10^{-16}$	Yes

[a] Calculated assuming that each water molecule can be ionized once.
[b] Assumed to be equal to the one of fused silica [20].
[c] The W_r value in Table 1 in Ref. [10].

gives rise to a positive phase shift.

In this model, $e_{free}^- \rightarrow e_{trap}^-$ is the hydration process, i. e., once the electron is trapped, it digs its own hole; it is introduced by the time dependence of the trap absorption $\omega_{trap}(t)$ that takes the hydration process $e_{trap}^- \rightarrow e_{hyd}^-$ into account, and we assume that the electron trap depth is a function of time:

$$\omega_{trap}(t) = \omega_{trap}^0 + (\omega_{hyd}^\infty - \omega_{trap}^0) \times \\ \times [1 - \exp(-t/\tau_{solv})], \quad (2)$$

where ω_{trap}^0 and ω_{hyd}^∞ are the respective absorption maxima of the trapped electron and the fully hydrated electron.

To produce the electron, we consider a 3rd-order multiphotonic absorption process [22] followed by a trapping process. The rate equations are then given by

$$\frac{dN^{free}}{dt} = \frac{\eta}{3} N_0 \sigma^3 I_p^3 - \frac{N^{free}}{\tau^{trap}},$$
$$\frac{dN^{trap}}{dt} = \frac{N^{free}}{\tau^{trap}}, \quad (3)$$

where N_0 is the total initial electron density of water, σ^3 is the 3rd-order multiphoton cross section, and η is the water ionization quantum yield.

The parameters for which the best fit is obtained for the phase shift (Fig. 2a) and absorption (Fig. 2b)

are summarized in Table. We emphasize that the set of parameters known from the literature (marked with "No" in Table) imposes very restricting constraints on the other parameters (marked with "Yes") and on the functional forms as well. Any small deviation of a parameter strongly deviates the fit from the "error bars". We estimate the range of validity of our inferred parameters better than 5 %, well in the range of expected values in Ref. [25].

Taking the solvation time τ^{solv} to be 450 fs, we find that, without any doubt, our results support not only the idea of a noninstantaneous solvation process (assumed to be a continuous shift in the present study) but also, for the first time, the importance of the free electron in the spectroscopic data. The passage through the resonance (when the trap position is equal to the laser wavelength) occurs after about 400 fs and explains the origin of the observed bump in the absorption kinetics. Both the phase shift and absorption are very well reproduced. The abrupt phase change around zero time delay can solely be explained by instantaneously formed species, i. e., the free electron inside the conduction band of water. The free electron induces the strong negative phase shift observed at early delay times. This result seems to contradict the findings on IR probe of the electron hydration process in [15], where an almost instantaneous electron attachment to a water molecule was found; but it is not. Indeed, that study was performed at relatively low pump power densities (a few GW/cm^2) while the present one is performed at extremely high power densities (a few TW/cm^2).

It is well known that water contains a large number of traps [26] that favor the electron attachment during the solvation process, as was recently demonstrated with first-principle molecular dynamics [27]. It was proposed that at least for low pump power densities, the lifetime of the free electron is less than 1 fs [28]. At high pump power densities, another mechanism operates. It can be proposed that the density of traps is not large enough compared to the number of electrons injected into the liquid ($9.7 \cdot 10^{19}$ cm^{-3}) and that part of free electrons have to wait for a cavity to be formed via the fluctuation of the liquid. We note that the measured excitation density is well below the total electron density, which validates the use of the Drude model.

In the study of the electron trap density in water [26], it was proposed to classify the traps as a function of their depth: deep traps that are favorable to electron localization ($E_{trap} < -0.83$ eV) and the rest, called shallow traps. The concentration of deep traps they found was 0.22 mol/l ($1.3 \cdot 10^{20}$ cm^{-3}). It is interesting to note that the number of injected electrons

is almost equal to the number of available traps estimated from classical molecular dynamics. It is therefore not very surprising that the observed hydration mechanism described in this paper differs substantially from the one described in previous publications. The trap energy fluctuations process is the result of water dynamics (i. e., thermal fluctuations in the liquid) that runs perpetually. In [26], two types of dynamics related to the energy trap fluctuations we observed: an ultrafast contribution associated to libration motions of water molecules and a slow motion (a few hundreds of femtoseconds).

The timescales described here are much like the ones observed for the frequency shift correlation function of the OH vibrator in water (50 and 650 fs) [29–31]. If we admit that the main step of trap formation (respectively, disappearance) is the breaking (respectively, formation) of an H bond, then we can propose that both rates are equal to the H bond lifetime, 700 fs [32]. Our trapping time is somewhat smaller than but comparable with the H bond lifetime and gives confidence that at high pump power densities, the limiting event is indeed the number of traps available. The relatively high value of ω_{trap}^0 has to be balanced with the fact that our "slow" trapping rate hinders part of the solvation process, which is not a single exponential as stated earlier. This indicates that when the conduction band of water is significantly populated, the electrons are preferentially trapped in deep traps. This fact is related somehow with the relatively small value of the reduced electron mass in the conduction band, which reflects a more pronounced metallic character of water when its conduction band is significantly populated.

This interferometric technique, used for the first time in liquid water, demonstrates that for high laser intensities, right after the injection process by an ultrashort pulse, the electrons remain free during about 230 fs while the local "lattice" reacts, rearanging itself to reach the well-known solvation cage state after near 450 fs. The new observation in this paper is the delayed localization of the aqueous conduction-band electrons, attributed to the saturation of pre-existing cavities in the liquid by the very large number of excited electron states created by the high-intensity laser. For such a high concentration, the time needed for an electron to find a trap increases due to the saturation of deep traps. The present study provides a solvation scheme that is fully relevant for radiation-induced track electron solvation dynamics [1] due to the high local concentration of ionization events.

REFERENCES

1. A. Mozumder, *Fundamental of Radiation Chemistry*, Academ. Press (1999).

2. K. D. Jordan and M. A. Johnson, Science **329**, 42 (2010).

3. K. R. Siefermann and B. Abel, Angewandte Chem., Int. Edition **50**, 5264 (2011).

4. R. Musat, G. Vigneron, D. Garzella et al., Chem. Comm. **46**, 2394 (2010).

5. H. A. Schwarz, J. Phys. Chem. **96**, 8937 (1992).

6. F. J. Webster, J. Schnitker, M. S. Friedrichs et al., Phys. Rev. Lett. **66**, 3172 (1991).

7. R. B. Barnett, U. Landman, and A. Nitzan, J. Phys. Chem. **90**, 4413 (1989).

8. M. Boero, M. Parrinello, K. Terakura et al., Phys. Rev. Lett. **90**, 226403 (2003).

9. R. Spezia, C. Nicolas, A. Boutin, and R. Vuilleumier, Phys. Rev. Lett. **91**, 208304 (2003).

10. F.-Y. Jou and G. R. Freeman, J. Phys. Chem. **83**, 2383 (1979).

11. E. J. Hart and J. W. Boag, J. Amer. Chem. Soc. **84**, 4090 (1962).

12. A. Staib and D. Borgis, J. Chem. Phys. **103**, 2642 (1995).

13. A. Migus, Y. Gauduel, J. L. Martin, and A. Antonetti, Phys. Rev. Lett. **58**, 1559 (1987).

14. F. H. Long, H. Lu, and K. B. Eisenthal, Phys. Rev. Lett. **64**, 1469 (1990).

15. R. Laenen, T. Roth, and A. Laubereau, Phys. Rev. Lett. **85**, 50 (2000).

16. M. Assel, R. Laenen, and A. Lauberau, J. Chem. Phys. **111**, 6869 (1999).

17. C. Silva, P. K. Walhout, K. Yokoyama, and P. F. Barbara, Phys. Rev. Lett. **80**, 1086 (1998).

18. A. Thaller, R. Laenen, and A. Laubereau, Chem. Phys. Lett. **398**, 459 (2004).

19. M. Tauber and R. Mathies, J. Amer. Chem. Soc. **125**, 1394 (2003).

20. P. Martin, S. Guizard, P. Daguzan et al., Phys. Rev. B **55**, 5799 (1997).

21. S. Pommeret, F. Gobert, M. Mostafavi et al., J. Phys. Chem. A **105**, 11400 (2001).

22. R. A. Crowell, R. Lian, I. A. Shkrob et al., J. Phys. Chem. A **108**, 9105 (2004).

23. S. Guizard, P. Doliveira, P. Daguzan, and M. Perdrix, Nucl. Instrum. and Meth. in Phys. Res. B **116**, 43 (1996).

24. M. Samoc, A. Samoc, and J. G. Grote, Chem. Phys. Lett. **431**, 4413 (2006).

25. D. Milam, Appl. Opt. **37**, 546 (1998).

26. J. Schnitker, P. J. Rossky, and G. A. Kenney-Wallace, J. Chem. Phys. **85**, 2986 (1986).

27. J. P. Renault, R. Vuilleumier, and S. Pommeret, J. Phys. Chem. A **112**, 7027 (2008).

28. D. Nordlund, H. Ogasawara, H. Bluhm et al., Phys. Rev. Lett. **99**, 217406 (2007).

29. M. Diraison, Y. Guissani, J.-C. Leicknam, and S. Bratos, Chem. Phys. Lett. **258**, 348 (1996).

30. C. P. Lawrence and J. L. Skinner, J. Chem. Phys. **118**, 264 (2003).

31. M. Pshenichnikov, A. Baltuka, and D. Wiersma, Chem. Phys. Lett. **389**, 171 (2004).

32. G. Gallot, S. Bratos, S. Pommeret et al., J. Chem. Phys. **117**, 11301 (2002).